J. Fluid Mech. (1985), *vol.* 150, *pp.* 183–201
Printed in Great Britain

Time-domain measurements in separated flows

By I. P. CASTRO
Department of Mechanical Engineering, University of Surrey, Guildford

(Received 2 May 1984)

This paper describes a sampling technique which is non-periodic, but also non-random, and which allows a pulsed wire anemometer to be used to obtain time-domain information in separated flows. Data free from aliasing can be obtained at frequencies considerably higher than that associated with the maximum possible (periodic) sampling rate achievable with a pulsed-wire probe. Autocorrelation and spectral data obtained in three quite distinct types of flow are presented, as a demonstration of the technique. Some of the data serve to emphasize the special character of separated flows. It is shown that in some circumstances it is possible to obtain spectral data that are adequate for estimating the turbulent-energy dissipation rate (provided that an inertial subrange exists). The measurement of all the terms necessary to examine the balance of turbulent energy in separated flows – or, at least, those terms which can be obtained by standard hot-wire anemometry in low-intensity flows – is therefore a distinct possibility.

1. Introduction

Over the last decade there have been a number of studies of highly turbulent flows involving regions of recirculation, in which the pulsed-wire anemometer originally described by Bradbury & Castro (1971) has been used. With the single exception of the work of Gaster & Bradbury (1976), hereinafter referred to as GB, all the measurements have been of time-averaged mean and fluctuating quantities. Whilst such information can be very instructive and is often difficult (and expensive) to obtain in any other way, there is increasing interest in the large-eddy structures of separated flows. Bradshaw & Wong (1972), for example, suggested that the large eddies present in the separated shear layer behind a rearward-facing step are 'torn in half' as reattachment is approached. They were unable to make direct length- or timescale measurements, however, and other workers have since disagreed about the fate of the large eddies (e.g. Hillier, Latour & Cherry 1983; Eaton 1984). Definitive conclusions can only be reached on the basis of spatial and autocorrelation measurements within the shear layer itself, but these are not possible using ordinary hot-wire anemometry because of the high turbulence levels.

One of the long-term aims of the turbulent-flow instrumentation work at the University of Surrey is therefore to develop means of obtaining such information. Because of our extensive experience of pulsed-wire anemometry it has been natural to use that instrument as the starting point, although it should be noted that laser–Doppler techniques have also been used recently to obtain some limited spectral measurements in separated flows (e.g. Restivo & Whitelaw 1978; Simpson, Chew and Shivaprasad 1981). Unlike the hot wire, the pulsed-wire anemometer is essentially a digital instrument which yields a single value of velocity every time the central pulsed wire is 'fired'. The finite (non-zero) time constant of the wire limits the

minimum interval between 'firings', since the wire must be allowed to cool between each sample. Periodic sampling could therefore only yield frequency information up to, typically, 50 Hz, and aliasing would distort spectral results at even lower frequencies. GB showed how random-sampling techniques could be used to increase the frequency resolution of the instrument. Essentially, they used Poisson-distributed time sequences, generated from a Gaussian white-noise source, to trigger the pulsed wire. Time delays less than the minimum allowed to prevent wire burn-out were suppressed and the autocorrelation function was obtained for all other lags using the slotting method described by Gaster & Roberts (1975). Measurements in the wake of a flat plate normal to an air stream were made, and Fourier transforms of the autocorrelations yielded velocity spectra that clearly showed the dominant vortex-shedding peak.

In the work described here, a rather different non-periodic sampling technique is used to obtain the autocorrelation. It has the advantage of being simple to implement on a microcomputer so that relatively rapid on-line estimates of the autocorrelation can be obtained without the necessity of hardware (or software) Poisson time-sequence generation.

Section 2, in addition to outlining the general experimental set-up, describes the technique in some detail. Examples of autocorrelation and spectral measurements in various flows are presented in §3. Some of these are interesting in their own right, since they illustrate some of the complexities of separated flows, but the major purpose here is to demonstrate the usefulness of the technique. Current work includes development of spatial correlation techniques – using two pulsed-wire probes. In flows where Taylor's hypothesis is clearly invalid this is a necessary development, since it is impossible to deduce lengthscale information from autocorrelations.

An additional motivation in the present work was the hope that it might be possible to obtain alias-free and sufficiently noise-free spectral data at the higher frequencies to allow estimates of the turbulent-energy dissipation rate to be made (assuming that an adequate inertial subrange exists in separated-flow regions). Since we have already shown that tolerably accurate Reynolds-stress measurements can be made (Castro & Cheun 1982), this would be a significant step towards being able to measure turbulent-energy balances in separated flows. This problem was not addressed by GB.

2. Experimental techniques

2.1. *The flows used*

The experiments were undertaken in the 0.2 m diameter axisymmetric jet rig and the 0.62×0.77 m blowdown wind tunnel in the Mechanical Engineering Department. In the former case, measurements were first made in the axisymmetric mixing layer 2.5 jet diameters downstream of the jet exit, at a Reynolds number based on jet diameter of at least 0.8×10^5. Secondly, a separated flow was generated by mounting a thin 0.1 m diameter disk centrally in the jet exit plane. The disk was held in place with four, symmetrically disposed, tensioned wires. Measurements were made at various locations in the wake of the disk – principally within the separated shear layer and at the location of the mean free stagnation point on the wake centreline.

In the latter case a 26 mm square-sectioned block spanned the shorter (horizontal) side of the tunnel on a false floor mounted about 100 mm from the tunnel floor. The upstream boundary layer was tripped near the leading edge of the false floor and the block was placed about 0.75 m downstream where δ/h, the ratio of boundary-layer thickness to body height in the absence of the body, was about 0.2. An earlier study

of this flow has been described by Castro (1981). Measurements were made in the near wake – principally in the reattachment region $13h$ downstream and near the centre of the reversed-flow region, $7h$ downstream.

2.2. *Instrumentation*

All the measurements were made using either standard hot-wire anemometry or pulsed-wire anemometry. The instruments were interfaced – via a 10 bit Prosser Scientific Instruments analogue-to-digital converter in the case of the hot wire – to the user port of a Commodore 6502-based PET microcomputer. DISA gold-plated hot-wire probes were used in conjunction with the PSI bridges and A/D converters. The latter included instrumentation amplifiers allowing d.c. offsets and gains to be applied to the bridge outputs before digitization, so enabling the maximum range of the A/D converter to be used. Inbuilt multiplexers allowed all 10 bits to be accessed by the computer. The pulsed-wire anemometer also has an inbuilt multiplexer, allowing the 12 bit time of flight information to be accessed, although in this work only the most significant 11 bits were used.

All probe calibrations were performed on-line, and look-up tables generated to allow rapid linearization during the measurement traverses. (This is a standard feature of the PSI and pulsed-wire software packages.) The standard software was used for measurements of mean and fluctuating quantities with either instrument. Typically sampling rates were 300 Hz and 100 Hz for the single hot wire and the pulsed wire respectively, so that averaging times of about 30 s – long enough to average the low frequencies sufficiently – led to sample sizes large enough to make statistical errors caused by a finite sample size insignificant.

2.3. *Autocorrelation measurements*

The autocorrelation function can be estimated from N data values of a periodically digitized signal using the standard relation:

$$R(m\,\Delta\tau) = \frac{1}{N}\sum_{n=1}^{N-m} u_n\,u_{n+m} \quad (m = 0, 1, 2, \ldots, M;\ M \ll N), \tag{1}$$

where $\Delta\tau$ is the time between successive samples. In a block of N samples there are fewer contributions to $R(\tau)$ for high values of m (long lag times) than for low, so the statistical accuracy of the $R(\tau)$ estimates falls with increasing m. For on-line correlation measurements it is usually best to take a series of blocks of data, each of N samples, and update $R(\tau)$ after each block. This avoids the requirement for extensive storage capacity. $R(\tau)$ would then normally be estimated from

$$R(m\,\Delta\tau) = \frac{1}{NK}\sum_{k=1}^{K}\sum_{n=1}^{N-m} u_n\,u_{n+m} \quad (m = 0, 1, 2, \ldots, N-1), \tag{2}$$

where K is the number of blocks. Only one contribution to the maximum lag ($(N-1)\,\Delta\tau$) value is available per block, so if accurate values of these are required a large number of blocks is necessary. The accuracy of the $R(\tau)$ estimates at the shorter lags would then often be unnecessarily high. In the present work, therefore, only one contribution for each lag value was used per block, so that $R(\tau)$ was computed from the K blocks of N samples by

$$R(m\,\Delta\tau) = \frac{1}{K}\sum_{k=1}^{K} u_0\,u_m \quad (m = 0, 1, 2, \ldots, N-1).$$

This also significantly reduces the required number of multiplications, and is

therefore particularly suitable for implementation on a microcomputer, since these do not generally have hardware arithmetic facilities (apart from add and subtract operations). $R(\tau)$ was updated for each m after every block of N samples had been obtained. We have found that 5000–20000 blocks is generally sufficient to obtain adequately smooth autocorrelation functions, provided an appropriate normalization is used. $R(\tau)$ is usually normalized by subtracting the square of the mean velocity and dividing by the mean square, i.e.

$$\tilde{R}(\tau) = (R(\tau) - \bar{U}^2)/\overline{u'^2},$$

but it is crucial to make a proper estimate of $\bar{U}$. An obvious approach would be to estimate $\bar{U}$ from

$$\bar{U} = \frac{1}{KN} \sum_{k=1}^{K} \sum_{n=1}^{N} u_{n,k},$$

i.e. to use *all* the sampled values. In principle this is correct if $KN \to \infty$, but it leads to totally unacceptable estimates in practical cases. Intuitively one might expect better estimates to be obtained if only those samples contributing to the particular $R(m\,\Delta\tau)$ value were used to estimate $\bar{U}^2$. This does, indeed, lead to much smoother autocorrelation functions. In the present work $R(\tau)$ was estimated from

$$\tilde{R}(\tau) \equiv \tilde{R}(m\,\Delta\tau) = \frac{R - \frac{1}{K}\sum_{k=1}^{K} u_0 \frac{1}{K}\sum_{k=1}^{K} u_m}{\overline{u_0'^2}}, \tag{3}$$

where u_0 is the first sample of each block and $\overline{u_0'^2}$ is given by

$$\overline{u_0'^2} = \frac{1}{K}\sum_{k=1}^{K} u_0^2 - \left(\frac{1}{K}\sum_{k=1}^{K} u_0\right)^2.$$

$\overline{u_0'^2}$ is used for convenience – the critical quantity as far as variability is concerned is the $\bar{U}^2$ estimate. It could be argued that since, in principle, the autocorrelation data will always be contaminated by a spike at zero lag, caused by random noise, normalizing by $\overline{u_0'^2}$ will lead to the random noise appearing in the spectrum. In the present work, however, it was found that sensible changes in the $R(0)$ value did not significantly affect the spectral results. Note that we did *not* use

$$\frac{1}{4K}\sum_{k=1}^{K} (u_0 + u_m)^2;$$

this might seem a reasonable alternative for $\bar{U}^2$ but leads to greater variability than the form given in (3). This can be readily demonstrated by writing $U_0 = \bar{U} + \epsilon_0$ and $U_m = \bar{U} + \epsilon_m$ and expanding each of the above expressions, noting that in general neither $\bar{\epsilon}_0$ nor $\bar{\epsilon}_m$ are zero.

It is worth noting that whilst the availability of hardware arithmetic would possibly make this a less efficient technique for obtaining $R(\tau)$ than the conventional approach of (1) or (2), there is no doubt that the latter may involve considerable redundancy and can give misleadingly smooth autocorrelation functions. For example, $u_n\,u_{n+m}$ and $u_{n+1}\,u_{n+1+m}$ would normally be highly correlated, particularly for the higher values of m (greater lag times). Arguably, therefore, it is pointless to include them both in obtaining the estimate for the mth mean cross-product.

For the hot-wire anemometry, the Prosser software was supplemented by routines allowing the autocorrelation function defined by (3) to be obtained. The internal

1 MHz clock of the computer was used for timing the lags, and all the time-consuming part of the data analysis was performed at machine-code level. Up to 256 samples (lags) per block, with lag times $\Delta\tau$ as low as about 120 μs, could be obtained. In a typical case of 64 samples per block with $\Delta\tau = 1$ ms/1000 blocks took about 110 s. If the intention in any particular measurement was to obtain the frequency spectrum by Fourier-transforming $R(\tau)$ then it was normally necessary to sample more rapidly (to minimize aliasing problems) and to obtain more samples per block. Sampling times were therefore correspondingly longer in such cases.

A possible alternative to Poisson sampling for estimation of autocorrelations using the pulsed-wire anemometer is to use a sequence of arithmetically increasing lag times. For example, taking an extremely simple case, if the minimum lag time ΔT were 5 ms and $R(\tau)$ estimates at lag intervals $\Delta\tau$ of 1 ms up to a maximum of 12 ms were required, the sampling sequence 5, 6, 7, 8, 9, 10, 11, 12 could be used, where the numbers refer to lag times, not sampling times. The latter would be 0, 5, 11, 18, 26, 35, 45, 56, 68 ms. This technique was discussed by Fagih (1980), who showed that the aliasing frequency in the spectrum obtained by transforming the resulting autocorrelation is $1/(2\Delta\tau)$. Periodic sampling, with a minimum lag time of ΔT, would reduce this to $1/(2\Delta T)$, and this is, of course, the attraction of non-periodic sampling techniques. Toy (1979) has successfully used the arithmetic-sequence method outlined above, but it has the distinct disadvantage of being relatively time-consuming. There are obvious redundancies: for instance, the lag time of 11 ms, in the above example, could be obtained from the first and third samples, without the necessity of the specific lag of 11 later in the sequence. In fact it is not difficult to show that a non-arithmetic sequence can be constructed to give all the lag values between 5 and 29 ms in almost the same total sampling period. A possible sequence of lag times is 5, 9, 7, 5, 5, 5, 5, 5, 6, 8, 5, 5, 5, 5 with a resulting sampling time sequence of 0, 5, 14, 21, 26, 31, 36, 41, 46, 52, 60, 65, 70, 75, 80. So the sampling time has increased by only 12 ms to 80 ms, but the resulting maximum lag value for which all the lower contributions are present (down to 5 ms) has increased from 12 ms to 29 ms. The sequence also contains $R(\tau)$ contributions at lags of 31, 32 and 34 ms, and the addition of two further samples (one in the centre and one at the end of the sequence) would enable the 30 and 33 ms lags to be obtained with an additional total sampling period of only 10 ms. Note that to obtain the 30–34 ms values with an arithmetic sequence requires an increase of 160 ms, on top of the necessary 425 ms required to obtain the 5–29 ms contributions!

Clearly there are significant advantages in ordering the sequence in some way other than arithmetically. Given a required maximum lag time T_p (usually chosen to ensure that $R(\tau)$ has decayed to zero), a minimum delay time ΔT and the required lag increment $\Delta\tau$, the problem is to order the sequence in such a way that all the lag contributions between ΔT and T_p are present but the total sampling period is a minimum. A simple algorithm which does just that was constructed and programmed (in BASIC), and the resulting sequence of delay times and sample pairs required to form each lagged cross-product were input, for the required T_p, ΔT and $\Delta\tau$, to the machine-code part of the autocorrelation software package. $\tilde{R}(\tau)$ was then estimated in a similar way to that described earlier.

A complicating factor for pulsed-wire measurements is that the anemometer produces occasional spurious time-of-flight readings which the software must reject. The velocity is set to zero for each 'bad' sample so that its contribution to all the sums is also zero. In the autocorrelation estimates it is important to keep track of

the number of these bad samples for each $m\Delta\tau$ values separately. The numerator of (3) becomes

$$\frac{1}{K_1}\sum_{k=1}^{K} u_0 u_m - \frac{1}{K_2}\sum_{k=1}^{K} u_0 \frac{1}{K_3}\sum_{k=1}^{K} u_m,$$

where $K_1 = K - S_{0m}$, $K_2 = K - S_0$, $K_3 = K - S_m$, and S_0 and S_m are the number of bad samples of u_0 and u_m respectively occurring in the K blocks. In general, S_{0m}, the number of bad contributions to the cross-product, satisfies $S_{0m} \geqslant S_0$, S_m and $S_{0m} \leqslant S_0 + S_m$, and must be counted separately. Failure to account properly for the bad samples can lead to highly increased variability in the $R(\tau)$ estimates, unless their total number is exceptionally small ($\ll 1\,\%$).

There remains the problem of estimating the missing lag values between 0 and ΔT. In the example discussed earlier $\tilde{R}(\tau)$ values at $\tau = 0, 1, 2, 3$ and 4 would be required. This has been discussed by GB and more fully by Stone (1978) and Fagih (1980). If the intention is simply to use the autocorrelation to obtain, say, an integral timescale, then a smooth curve drawn 'by eye' between $\tilde{R}(0) = 1.0$ and the available $\tilde{R}(\tau)$ values will almost always be sufficient. If a cosine transform is to be performed to obtain the frequency spectrum then this will not necessarily be adequate. The above authors discuss the use of maximum-entropy theory to deduce bounds on the missing $\tilde{R}(\tau)$ values, but in practice it is not always possible to use the latter method satisfactorily because of the relatively noisy data produced by a pulsed wire and the number of missing values required. This is discussed further in the following sections.

The autocorrelation techniques described above enable, say, 64-point autocorrelations with $\Delta\tau = 1$ ms to be obtained in, typically, 260 s/1000 blocks. Most of the increase in sampling time over that required for an equivalent periodically sampled hot-wire measurement (110 s/1000 blocks) is the inevitable result of the minimum-delay-time constraint. Some adjustment of the anemometer hardware and the reduction in the diameter of the pulser wire (reducing the wire time constant) has allowed ΔT to be reduced to a minimum of about 4.5 ms. In regions of low mean velocity and high intensity, however, considerably higher values of ΔT are necessary, as discussed later.

A final point concerns the possible influence of the imperfections in the pulsed-wire probe's yaw-and-pitch response. These were discussed in the context of the measurement of mean and mean-square velocities by Castro & Cheun (1982). It is very difficult to quantify errors in autocorrelation and spectral measurements. Whilst the area under the spectrum will be in error by an amount which can be estimated (see Castro & Cheun 1982), since this is equivalent to the mean square of the signal, it is not obvious how the imperfect yaw response will affect the spectral shape. Detailed estimates would require information concerning the spectral content of the flow *angle*. However, it is thought that errors arising from signal noise and finite sample and block sizes will usually dominate.

3. Results and discussion

3.1. *The axisymmetric mixing layer*

These experiments were undertaken essentially to validate the technique described in §2 and to check on the satisfactory operation of the software. Figure 1 is a sketch of the flow. Initial measurements confirmed that the mixing layer grew at the expected rate and had a turbulence structure similar to that discussed in the literature (at least as far as the distribution of the Reynolds stresses was concerned). Figure 2(*a*)

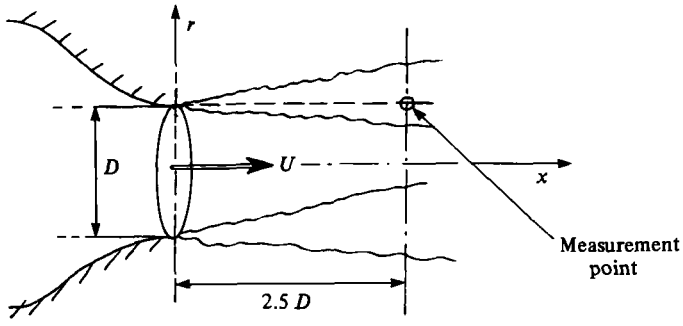

FIGURE 1. Sketch of the axisymmetric-jet rig.

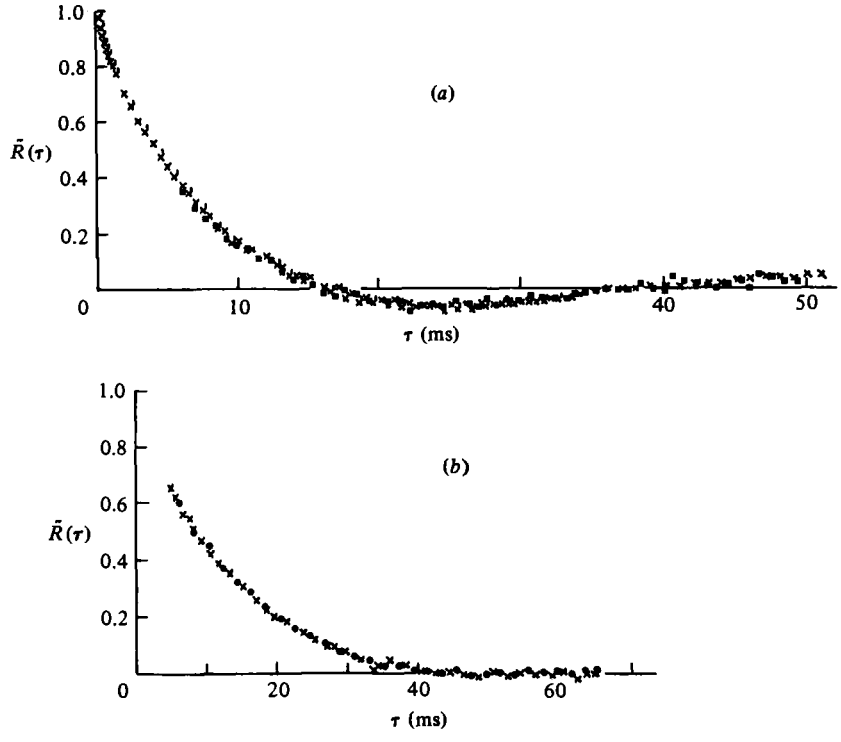

FIGURE 2. Autocorrelations in the axisymmetric mixing layer. For clarity, not all the data points are shown. $x/D = 2.5$, $r/D = 0.5$. (*a*) ×, 64 lags of $\Delta\tau = 1$ ms; ✕, 256 lags of $\Delta\tau = 133$ μs (hot wire). ■, 64 lags of $\Delta\tau = 0.768$ ms (pulsed wire, $\Delta T = 6$ ms). $U_r = 10.8$ m/s. (*b*) ●, 32 lags of $\Delta\tau = 2$ ms; ×, 128 lags of $\Delta\tau = 0.51$ ms. Pulsed-wire data. $U_r = 5.24$ m/s.

shows measured autocorrelation functions at $x/D = 2.5$, $r/D = 0.5$ – the mixing layer centreline – and an exit velocity of 10.8 m/s corresponding to $Re_D = 1.5 \times 10^5$. Two periodically sampled hot-wire autocorrelations are shown, one with 64 lags and $\Delta\tau = 1$ ms and the other with 256 lags and $\Delta\tau = 133$ μs. In both cases the bridge output was filtered at about 5 kHz. The pulsed-wire autocorrelation results shown were obtained with $\Delta T = 6$ ms and $\Delta\tau = 0.768$ ms (64 points, but with the first 8 missing). Good agreement between all three distributions is evident but the pulsed-wire data show rather more variability. By measuring the area under the positive

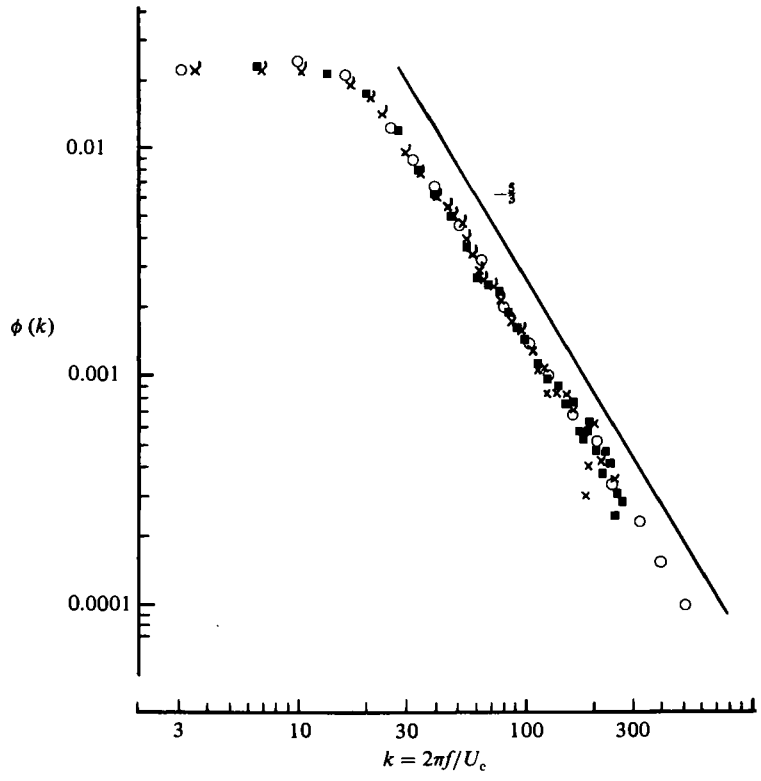

FIGURE 3. Energy spectra from autocorrelation data at $x/D = 2.5$, $r/D = 0.5$; $U_r = 5.2$ m/s. ×, ×, hot wire; ■, pulsed wire. ○, from analogue hot-wire frequency measurements.

portion of the $\tilde{R}(\tau)$ curve and invoking Taylor's hypothesis, a longitudinal integral scale given by $L_x = 0.074x$ was deduced.

Increasing the flow timescales by reducing the exit velocity enables correspondingly higher values of maximum $\tilde{R}(\tau)$ to be obtained from the pulsed wire. This is demonstrated in figure 2(*b*), which shows two pulsed-wire autocorrelations obtained at the same location as before but with a jet velocity of 5.24 m/s. Agreement with hot-wire results (not shown) was again good, and the resulting integral scale was close to its previous value. However, there are evidently some Reynolds-number effects since the negative loop in the correlation is much less pronounced at the lower velocity.

A fast-Fourier-transform routine (written in machine code) was used to obtain energy spectra from the hot-wire autocorrelations at the lower jet velocity, and these are shown in figure 3, compared with an analogue spectrum obtained using a Bruel & Kjaer frequency analyser. For frequencies up to about 60 Hz ($k = 2\pi f/U_c \approx 100$) the plotted results are from a transform of a 64 point, $\Delta\tau = 1$ ms autocorrelation, extrapolated to 256 points by the addition of zeros and then linearly interpolated to provide 512 points at 0.5 ms intervals. At higher frequencies an autocorrelation of 256 lags with $\Delta\tau = 0.25$ ms interpolated to 512 points ($\Delta\tau = 0.125$ ms), was used. In this case the analogue signal was filtered at 1 kHz. These latter points naturally show less influence of aliasing, but there is an inevitable increase in variability of the spectral data at high frequencies. Note that no digital filtering or smoothing has been employed, so these are 'raw' transformed results. Whilst filtering certainly

produces smoother data, it could never be guaranteed to give the correct $\phi(k)$ data at the higher frequencies unless the filter characteristics were chosen to force the correct behaviour! It should be noted that for an autocorrelation of the form $e^{-\tau}$, which has a spectrum that rolls off like f^{-2} at high frequencies, transformed data begins to deviate from that roll-off at frequencies around $\frac{1}{3}$ of the aliasing frequency. Since turbulent spectra roll off like $f^{-\frac{5}{3}}$ (until the dissipation frequency range) an even greater aliasing effect (for unfiltered signals) can be expected.

It is also important to note that the addition of random noise with a peak-to-peak amplitude of only 1 % to a correlation of the form $e^{-\tau}$ – a crude simulation of the presence of variability on the correlation estimates – leads to significant noise on the spectrum after less than two decades of energy decay. In many practical applications this would not be too significant, but in turbulence work it is often desirable to plot spectra in the form used in figure 3 – to look for a $-\frac{5}{3}$ region, for example – so particularly smooth autocorrelations are required. This requires a very large number of blocks, though the problem would undoubtedly be reduced if more than one of the available sample pairs in each block were used to update the $\tilde{R}(\tau)$ estimate for each lag. As indicated earlier, unless hardware arithmetic were available, this would significantly increase the total sampling time even without any increase in the number of blocks.

The pulsed-wire spectral data shown in figure 3 was obtained from the 128 point 0.5 ms lag autocorrelation shown in figure 2(*b*), with the initial eight missing points supplied by drawing a smooth curve through $\tilde{R}(0) = 1$ and the actual data. The minimum delay time was 5 ms. It would in this case be possible to draw a feasible $-\frac{5}{3}$ line through the data, but again noise becomes significant for $k \approx 200$ (corresponding to a frequency of about 100 Hz). Now if periodic sampling with the same delay time of 5 ms were employed, this frequency would correspond to the aliasing frequency, so the spectral data would have deviated substantially from the $-\frac{5}{3}$ line by that point. There has therefore been a significant benefit in using the ordered sampling scheme, as expected. It is clear, however, that even if the aliasing frequency for the latter is given by $1/(2\Delta\tau)$ (1 kHz) – and we have not proved, for the present non-arithmetic sequence, that this *is* the case – noise has prevented the full benefits being obtained. The increased variability of the pulsed-wire autocorrelations and spectra, compared with those obtained with a hot wire, is almost certainly due to the lower signal/noise ratio of the former instrument, rather than the non-periodic sampling technique. Initial experiments with non-periodic sampling of a hot-wire signal yielded data whose variability seemed little different to that obtained by periodic sampling.

Finally, it should be noted that small changes in the estimated missing lag values of $\tilde{R}(\tau)$ did not seem to affect the spectral results significantly. The level of noise in the pulsed-wire autocorrelation and the fact that eight values were needed, prevented the successful application of maximum-entropy methods. An 'eyeball' method was therefore the only option available, but seemed quite adequate.

These results sufficed to satisfy us that the software was working correctly and that the non-arithmetic sampling sequence could be used to obtain reasonable spectra up to frequencies at which noise became significant.

3.2. *The axisymmetric wake*

This flow is sketched in figure 4(*a*). From pulsed-wire mean-velocity measurements the free stagnation point on the symmetry axis was found to be at $x/D \approx 1.65$. Figure 4(*b*) shows lateral distributions of mean velocity and longitudinal turbulence energy at $x/D = 1.0$ and a reference velocity U_r, of about 4.5 m/s. U_r was measured

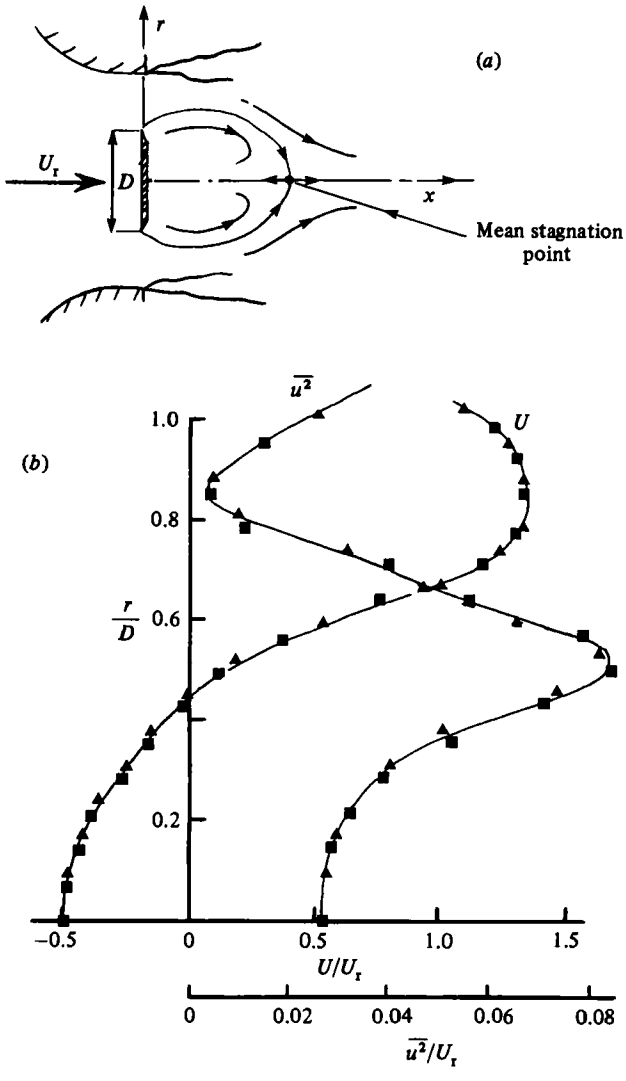

FIGURE 4. (*a*) Sketch of the axisymmetric separated wake flow. (*b*) Velocity and turbulence energy at $x/D = 1.0$. ▲, ■, data from opposite sides of the axis of symmetry.

in the jet exit plane in the absence of the disk but with the same settling-chamber static pressure. Pulsed-wire autocorrelations of the U-component velocity are shown in figure 5 for three different lateral locations on $x/D = 1.0$: the centreline ($r = 0$), where the mean velocity was negative and equal to about half the reference value, $r/D = 0.45$, where the mean velocity was zero, and $r/D = 0.6$, roughly the centre of the separated shear layer.

The autocorrelation at $r/D = 0$ looks quite 'normal' (figure 6*a*), and since the local turbulent intensity was only about 30% at that location, it is possible to estimate the integral scale, using Taylor's hypothesis. Taking the convection velocity as the local mean value, $L_x \approx 18$ mm, which might seem surprisingly low since the disk diameter is 100 mm. However, on the assumption that the separated mixing layer develops roughly like the ordinary mixing layer discussed in §3.1, this is roughly the integral scale that would be obtained in the region of the free stagnation point.

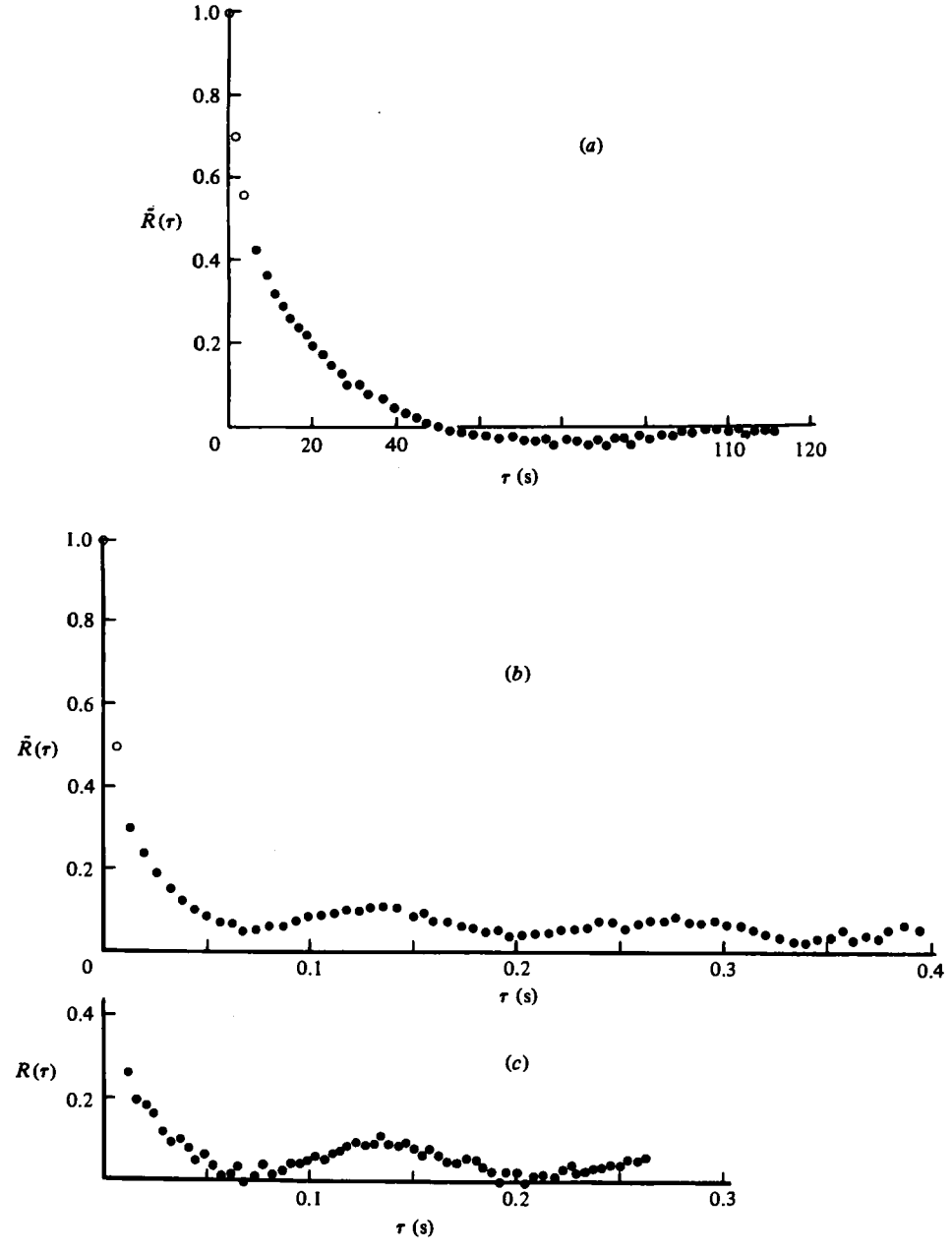

FIGURE 5. Pulsed-wire autocorrelations in separated wake at $x/D = 1.0$; ●, measured data; ○, interpolated values. (*a*) 64 lags of 2 ms; $\Delta T = 6$ ms, $r/D = 0$. (*b*) 64 lags of 6 ms; $\Delta T = 12$ msec, $r/D = 0.45$. (*c*) 64 lags of 4 ms; $\Delta T = 12$ msec, $r/D = 0.60$.

The flow within the cavity region may therefore have lengthscales typical of the flow being returned to it in the stagnation region, although spatial-correlation measurements would be needed to confirm such a conclusion.

Although there is a small negative loop in the autocorrelation, there is no real evidence of any strong periodicity in the flow. However, autocorrelations in the separated shear layer itself do contain an obvious periodic component – figures 5 (*b*, *c*).

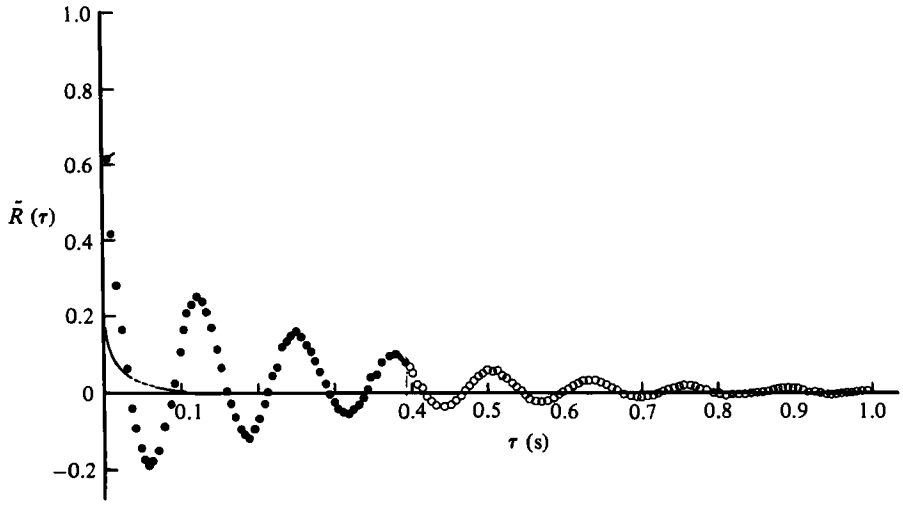

FIGURE 6. v-component autocorrelation at the free stagnation point: $x/D = 1.65$, $r/D = 0$. ●, 64 lags of 6.1 ms, $\Delta T = 12$ ms. ○, data extrapolated by maximum-entropy methods (up to 256 lags; only the first 192 are plotted here). ◐, interpolated values; ——, u-component autocorrelation.

It is also apparent that a significant low-frequency content is present since the general decay of the correlation is very slow. This is particularly noticeable at $r/D = 0.45$ (figure 5*b*), but since the mean velocity is zero at that point it is not possible to interpret the autocorrelation in terms of lengthscales. The periodic nature of the flow was most clearly demonstrated by the autocorrelation of the V-component velocity fluctuation at the stagnation point, $x/D = 1.65$, $r/D = 0$. This is shown in figure 6, along with the U-component correlation, which is shown as a smooth line drawn through the (unplotted) data points. These results are reminiscent of the results of GB obtained in the wake of a two-dimensional normal flat plate. Note again that the V-component autocorrelation indicates significant low-frequency energy – the decaying oscillation (arising from the periodic shedding of ring vortices from the edge of the disk) is superimposed on a very slowly decaying autocorrelation.

The data in figure 6 were obtained from a 64 point, $\Delta\tau = 6.14$ ms sequence, with a minimum delay ΔT of $2\Delta\tau$. Because the mean velocity was zero at this location, the pulsed-wire time constant was on average considerably higher than elsewhere in the flow, so it was not possible to reduce this minimum delay without a large increase in the number of 'bad' samples arising from the additional 'hot-wire anemometry' of the sensor signals before the heat tracer finally decayed. The sampling time per block was about 0.5 s, so the 20000 blocks used to obtain the autocorrelation required over $2\frac{1}{2}$ hours! Since the autocorrelation had not decayed to zero even after a lag of 0.39 s (64×6.14 ms), a direct Fourier transform would give inadequate spectral data. $\tilde{R}(\tau)$ was therefore extended to 256 points using maximum-entropy methods, as discussed by GB, Stone (1978) and Fagih (1980). The additional $\tilde{R}(\tau)$ data (up to the 192 lag) is included in figure 6, and figure 7 shows the resulting spectral data, which contains the expected Strouhal peak at $k \approx 11$, corresponding to a frequency of about 7.9 Hz and a Strouhal number fD/U_r, of about 0.17.

Obtaining adequate spectral data at wavenumbers higher than about 55 ($f = 40$ Hz; $1/(2\Delta\tau)$ in this case was about 80 Hz) would clearly necessitate much smaller delay values ($\Delta\tau \ll 6$ ms), but this presents a fundamental difficulty in regions

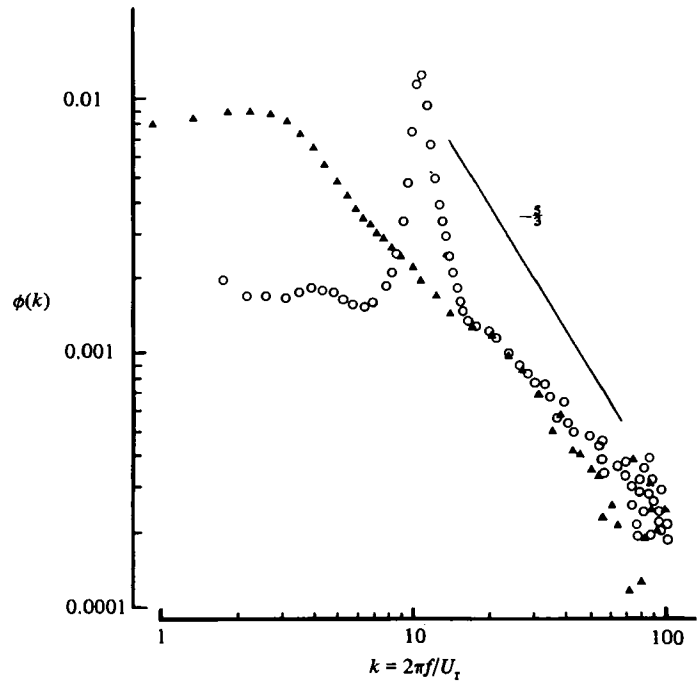

FIGURE 7. Energy spectra: ○, from v-component autocorrelation (figure 6). ▲, from u-component autocorrelation (figure 5a).

of very low mean velocity, since a typical heat-tracer convection time could then be of the same order, or higher, than $\Delta\tau$. In the present case, for example, an instantaneous velocity of around 1 m/s (corresponding to about half of the actual standard deviation of the velocity fluctuation) would correspond to a convection time of about 1 ms, with lower velocities having correspondingly greater heat-tracer convective times. Under these circumstances it would not be reasonable to expect to be able to obtain accurate spectral data at frequencies up to $1/(2\Delta\tau)$.

Obtaining sensible spectra from the autocorrelations shown in figures 5(b, c) would clearly be impractical, since extrapolation until $\tilde{R}(\tau)$ had decayed to zero would be required; the variability in the data makes maximum-entropy extrapolation impossible. In addition, the very low initial values of $\tilde{R}(\tau)$ would make proper estimation of the missing $\tilde{R}(\tau)$ values very difficult. However, the transform of the data in figure 5(a) is included in figure 7, from which it is evident that reasonable spectral estimates were possible for that case. There is a slight hump in the spectra around a k corresponding to twice the shedding frequency. Any possible $-\frac{5}{3}$ region is obscured by noise, which becomes significant at frequencies much lower than was the case in the ordinary axisymmetric mixing-layer measurements described previously (see figure 3). This is almost certainly caused by the increased variability in the correlation data, but in view of the limitations caused by the finite heat-tracer convection time, mentioned earlier, there would seem to be little point in attempting to reduce this variability.

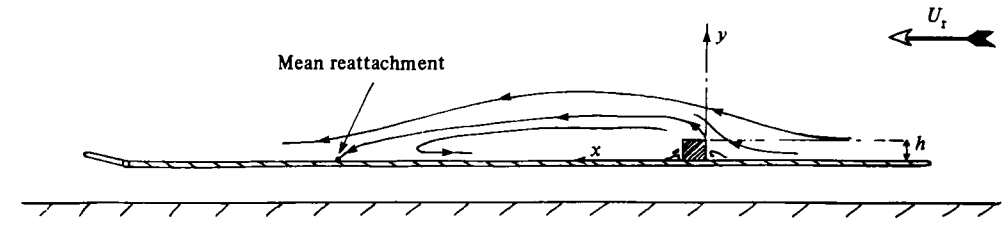

FIGURE 8. Sketch of the two-dimensional separated wake flow.

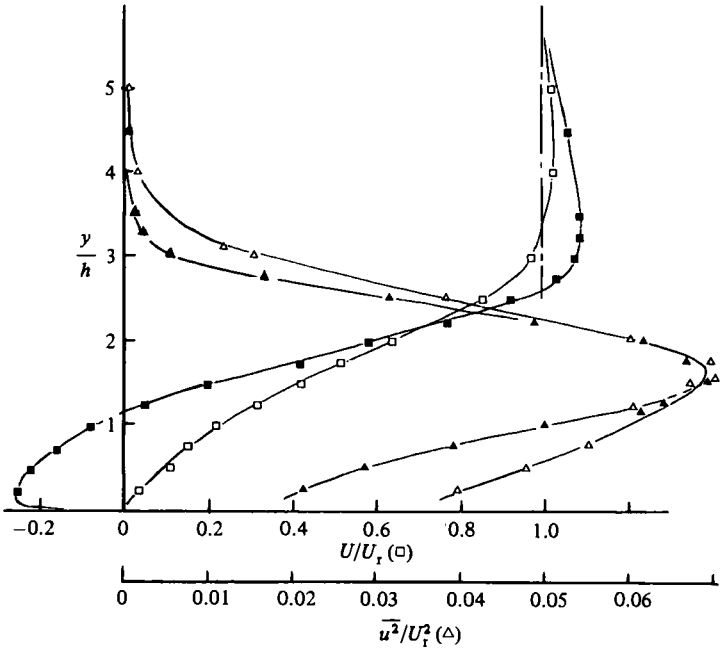

FIGURE 9. Mean velocity (□, ■) and turbulence energy (△, ▲) at $x/h = 7$ (closed symbols) and $x/h = 13$ (open symbols), in the wake of the square-section block (figure 8).

3.3. *The two-dimensional separated wake*

Previous work has shown that, unlike the flow discussed in §3.2, the wake of a surface-mounted two-dimensional body in a boundary layer contains no strong periodicity (Castro 1981). The final examples are of measurements made in such a flow; figure 8 is a sketch of the experimental set-up. Velocity and surface-pressure measurements showed that mean-flow reattachment occurred at $x/h = 13$, where h is the body height and x is measured from the front face of the block. Figure 9 shows the mean velocity and longitudinal turbulence-energy variations at $x/h = 7$ and 13 for a free-stream velocity of 8 m/s, corresponding to a body Reynolds number of 1.4×10^4. A number of pulsed-wire autocorrelations were obtained at these two axial stations, and some of these are shown in figure 10.

In all cases it is possible to estimate integral *time*scales, and these are not without interest. Figure 11 shows $T_x U_r/\zeta_w$, plotted against $(y-y_0)/\zeta_w$. T_x is the area under

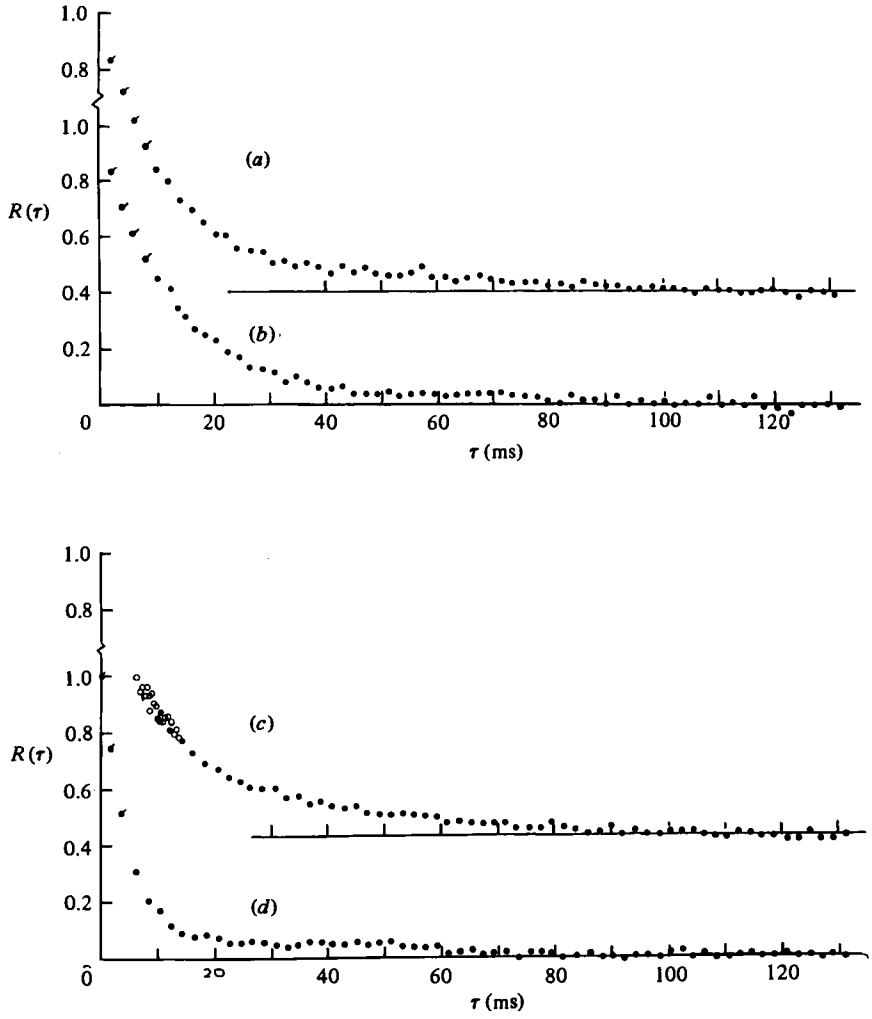

FIGURE 10. Pulsed-wire autocorrelations in the wake of the square-section block: ●, 64 lags of 2.07 ms; ◐, interpolated data. (*a*) $x/h = 13$, $y/h = 0.25$; (*b*) 13, 1.0; (*c*) 7, 0.25; ○, from results of a 128 lag, $\Delta\tau = 0.25$ ms autocorrelation; (*d*) $x/h = 7$, $y/h = 2.4$.

the autocorrelation and ζ_w is the vorticity thickness of the separated shear layer, defined in the usual way as

$$\left(\frac{\partial(u/U_r)}{\partial y}\bigg|_{\max}\right)^{-1}.$$

y_0 is the shear-layer centreline, defined arbitrarily as the location where the longitudinal turbulence energy is a maximum. The substantial increase in timescales over those typical of an ordinary mixing layer (also shown in the figure) cannot be solely attributed to the effect of normalizing by U_r rather than, say, the local mean velocity. Taking the local mean velocity as the convection speed, $T_x U_c/\zeta_w$ is also shown on figure 11. (Whilst Taylor's hypothesis can have no meaning in regions of low mean velocity and high turbulence intensity, it is probably a reasonable way of deducing lengthscales for $y \gtrsim y_0$). This latter timescale is higher than the ordinary mixing-layer values by about a factor of four at $x/h = 7$ near the shear-layer

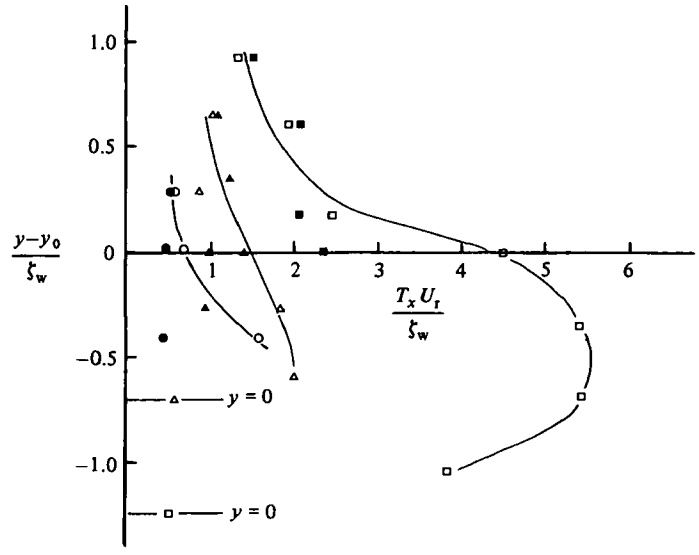

FIGURE 11. Variation of timescales across the separated mixing layer. Closed symbols are $T_x U_c/\zeta_w$. ○, axisymmetric mixing layer; △, $x/h = 13$; □, $x/h = 7$. Note the location of the wall ($y = 0$) in the latter two cases.

centreline, but the factor falls to about two near reattachment. Full discussion of this aspect of the results is not appropriate here, but, in any case, a proper interpretation requires more data than are currently available. It does seem, however, that the turbulent structure differs significantly from that of a classic mixing layer. Shear-stress measurements in a separated shear layer suggests the same conclusion (Castro & Cheun 1982).

Figure 12 shows a few of the spectra obtained from the autocorrelation data. Most of the latter were 64 point, 2 ms lag, results with ΔT, the minimum time delay, varying between 6 and 10 ms depending on the local mean velocity. $\tilde{R}(\tau)$ had decayed to zero in all cases, so the correlations were extrapolated by the addition of zeros to generate more resolution at low frequencies. It is encouraging that, even at $x/h = 13$, $y/d = 0.25$, where the mean velocity is only about 4% of the reference value (see figure 9*a*), a quite respectable spectrum is obtained, from which it would be possible to estimate the turbulent-energy dissipation rate since almost a decade of $-\frac{5}{3}$ subrange is apparent: it is not, in this case, 'hidden' by a dominant frequency component. The spectral data for $x/d = 7$, $y/d = 0.25$ are a little more scattered, but collapse remarkably well onto the $x/d = 13$, $y/d = 0.25$ results; the integral timescale is very similar at these two locations (but, since ζ_w is very different, normalized values are not the same, figure 11).

Some of the autocorrelations suggest the presence of two dominant but separated timescales; figures 10(*b*, *d*) are examples. The spectrum obtained for the latter case is also shown in figure 12. This is for a location in the outer half of the separated shear layer where, in addition to the energy present in the range corresponding to the usual energy-containing scales in a mixing layer, there is a significant amount of lower-frequency energy present ($k \lesssim 7.5$, $f \lesssim 5$ Hz, equivalent to a Strouhal number based on h and U_r of 0.03). There are insufficient data available to indicate whether this very-low-frequency component is present throughout the flow, but such a feature would be consistent with the recent results of Hillier *et al.* (1983), who found a similar

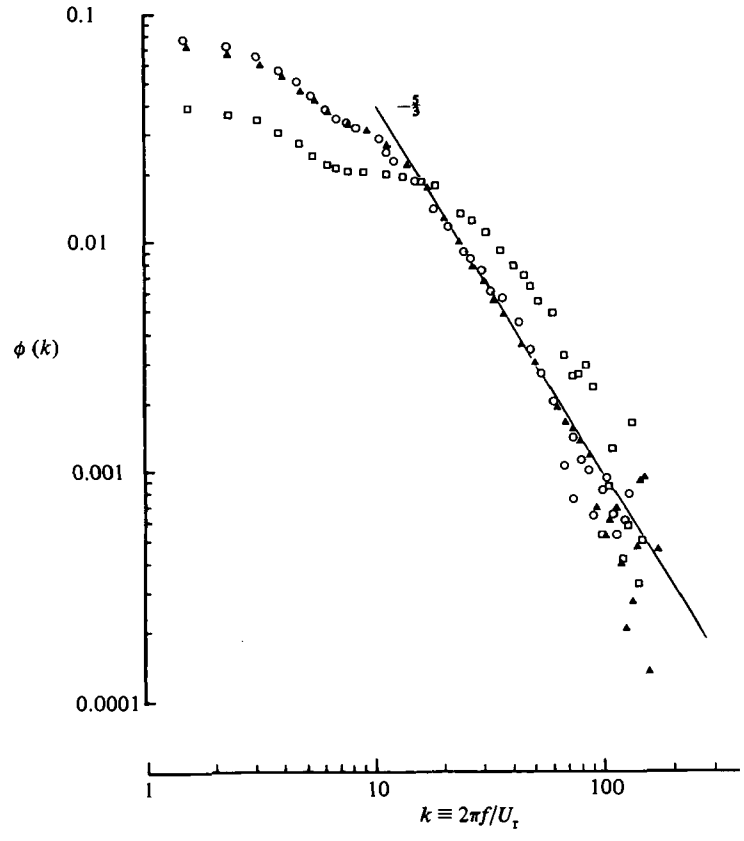

FIGURE 12. Energy spectra from pulsed-wire autocorrelations: ▲ $x/h = 13$, $y/h = 0.25$ (figure 10*a*); ○, 7, 0.25 (figure 10*c*); □, 7, 2.4 (figure 10*d*).

low-frequency component in hot-wire data taken at the outer edge of a separated shear layer.

Some autocorrelations of 128 points with $\Delta\tau = 0.25$ ms were also obtained, and an example is included in figure 10*c*, for $x/h = 7$, $y/h = 2.4$. For clarity, only some of the data have been plotted, but it is evident that the variability is significant. Now in this case the heat-tracer flight time corresponding to the mean velocity was about 0.5 ms so, as discussed in §3.2, lag times $\Delta\tau$ as low as 0.25 ms could not possibly provide meaningful data at frequencies of the order $1/\Delta\tau$. This is almost certainly the reason for the increased variability of the data in this case, and is a further example of the fundamental limitations discussed earlier. A typical probe has wire spacings of about 1.5 mm, so flight times are about $1.5/U$ ms, where U is the instantaneous velocity. There is consequently an inevitable frequency limit of around $U/1.5$ kHz (if U is in m/s), and in flows where U can be very low, or even zero, this clearly must impose severe restrictions on the upper frequency for uncontaminated spectral data.

4. Conclusions

The results presented in this work have demonstrated the usefulness of a pulsed-wire anemometer in obtaining autocorrelation data in separated flows. By using an

ordered (non-periodic) sampling scheme a relatively cheap microcomputer can be used to control the anemometer and perform on-line autocorrelation measurements much more quickly than is possible with an arithmetic sampling sequence and more conveniently than the random-sampling technique discussed by Gaster & Bradbury (1976). The availability of a fast-Fourier-transform code for the particular microcomputer used also allows spectral data to be easily obtained (1024 points in 26 s). If the flow is one that contains dominant periodicities, these can be easily resolved by the pulsed-wire aneomometer, as shown by Gaster & Bradbury (1976), but in these circumstances the combination of high-energy components at a specific frequency and the inevitable noise on the autocorrelation data will often prevent spectral data in the turbulent inertial subrange (if one exists) from being obtained with sufficient accuracy to allow estimation of energy-dissipation rates.

However, in separated flows that do not contain strong periodic energy components, it does seem possible to obtain spectral data adequate for this latter purpose, although, in regions of very low mean velocity, probe resolution limitations will sometimes prevent this. Integral-timescale measurements usually present no difficulty, but clearly the deduction of lengthscale information depends on the applicability of Taylor's hypothesis: in a separated flow the latter is of dubious value.

Since the inherent noise/signal ratio of a pulsed-wire anemometer is significantly higher than that of the classic hot wire, time-domain data of the kind discussed here usually have rather more variability for given sample sizes, but our results have shown this is not an overwhelming difficulty. The pulsed wire is certainly the cheapest way of obtaining such data: laser anemometry is much more expensive and arguably more difficult to use effectively to obtain time-domain information in separated (and other) flows characterized by very high turbulent intensities.

Understanding the physics of such flows clearly requires more information on the spatial extent of the various eddy structures, and current work therefore includes efforts to enable measurement of spatial velocity correlations (with variable time delay) in separated flows.

Useful discussions with Dr L. J. S. Bradbury, Dr M. Gaster and Mr P. Inman are gratefully acknowledged. Thanks are due to Dr T. Sweeting, of the Mathematics Department, University of Surrey, for help in producing the algorithm to determine the required non-periodic time sequences. The work would have been impossible without the technical skill of Mr T. Laws in probe construction and the help of the staff in the Mechanical Engineering Departmental Workshop. Grateful thanks are therefore also extended to them.

REFERENCES

Bradbury, L. J. S. & Castro, I. P. 1971 A pulsed-wire technique for measurements in highly turbulent flows. *J. Fluid Mech.* **49**, 657.

Bradshaw, P. & Wong, F. W. F. 1972 The reattachment and relaxation of a turbulent shear layer. *J. Fluid Mech.* **52**, 113.

Castro, I. P. 1981 Measurements in shear layers separating from surface mounted bluff bodies. *J. Wind Engng Ind. Aero.* **7**, 253.

Castro, I. P. & Cheun, B. S. 1982 The measurement of Reynolds stresses with a pulsed-wire anemometer. *J. Fluid Mech.* **118**, 41.

Eaton, J. K. 1984 Turbulence structure and initial-condition effects in a reattaching mixing layer. (Private communication).

FAGIH, N. 1980 Some studies of random signal analysis using simulated data. Ph.D. thesis, University of Surrey.

GASTER, M. & BRADBURY, L. J. S. 1976 The measurement of the spectra of highly turbulent flows by a randomly triggered pulsed-wire anemometer. *J. Fluid Mech.* **77**, 499.

GASTER, M. & ROBERTS, J. B. 1975 Spectral analysis of randomly sampled signals. *J. Inst. Maths Applics* **15**, 195.

HILLIER, R., LATOUR, M. E. M. P. & CHERRY, N. J. 1983 Unsteady measurements in separated-and-reattaching flows. Paper presented at Turbulent Shear Flows 4, Karlsruhe, September 1983.

RESTIVO, A. & WHITELAW, J. H. 1978 Turbulence characteristics of the flow downstream of a symmetric plane sudden expansion. *Trans. ASME* I: *J. Fluids Engng* **100**, 308.

SIMPSON, R. L., CHEW, Y.-T. & SHIVAPRASAD, B. G. 1981 The structure of a separating turbulent boundary layer. Part 2. Higher-order turbulence results. *J. Fluid Mech.* **113**, 53.

STONE, P. 1978 Use of the autocorrelation matrix in spectral analysis. Ph.D. thesis, University of Surrey.

TOY, N. 1979 The use of arithmetic sampling sequences for estimation of autocorrelations using a pulsed wire anemometer. Private communication.